CENTRAL Z_{eff} MEASUREMENTS WITH A NEW PHA DIAGNOSTIC AND ITS FURTHER APPLICATIONS ON ASDEX UPGRADE

D. O. Bolshukhin, R. Neu, M. Yu. Kantor*, B. Kurzan
and ASDEX Upgrade Team

Max-Planck-Institut für Plasmaphysik, EURATOM-Association, Garching, Germany
** Ioffe Institut, RAS, Politekhnicheskaya 26, St. Petersburg, 194021 Russia*

Operation principles and setup

A Pulse Height Analysis (PHA) diagnostic with a recently introduced Silicon Drift Detector (SDD) [1] was used at ASDEX Upgrade for the analysis of the central x-ray emission in the energy range from less than 1 keV up to 20 keV. The detector body is a 300 μm thick silicon crystal with 5 mm^2 surface. An electric field with a strong component parallel to its surface is applied by a system of field rings. The field rings are attached to the backside of the crystal (see Fig.1). In the center of the crystal a charge collecting structure is placed. It consists of an on-chip FET-transistor surrounded by an anode, which is connected to the gate of the FET by a short metallic strip. The extremely low anode capacity of $C = 200fF$ allows the measurement of X-ray spectra at very high count rates above 10^5 s^{-1} and short shaping times below 0.25 μs already at room temperature. The energy resolution of 150 - 160 eV at a photon energy of 6 keV, which approaches that of a liquid N_2 cooled Si(Li) detector, is reached with single stage Peltier cooling only. Due to the on-chip electronic no microphony effects disturb the signal. Incoming X-ray photons produce a number of free electrons in the detector body, which is proportional to the photon energy. In the applied electric field the free electrons produced by each single photon drift towards the anode and cause short charge pulses. The output signals of the FET are the amplified charge pulses. After further amplification by a charge sensitive amplifier the pulses are stored into a histogram memory with 1024 channels. The line of sight of the PHA diagnostic lies 11 cm above the mid-plane of the plasma vessel and crosses the plasma center for most of the discharge scenarios. The line of sight is shaped by the collimating system equipped with the set of variable diaphragms from 0.05 mm up to 6.00 mm in diameter, which allows the adjustment of the incoming photon flux within four orders of magnitude. A set of five Be foils from 2 μm up to 1000 μm thickness allows to set the low energy edge of the incoming radiation within the energy range from 0.5 up to 5 keV. The energy calibration of the PHA was performed by using known characteristic lines (Ar, Fe, Si) of spectra measured at ASDEX Upgrade. The quantum efficiency of the detector was determined as a product of a geometry factor with the energy dependent filter transmission and adsorption of the detector body, namely $\eta_{det} = T_{Be_{filt}} T_{window} T_{Si_{dead-layer}} A_{Si_{300\mu m}} c_{geom}$. Absolutely measured Fe lines at 6.4 keV were used to cross check the ab initio calibration of the Multi Bragg Spectrometer [2] having almost the same line of sight as PHA. The comparison of line intensities measured with both systems showed an agreement within 20 %.

Experimental

Emission spectra in the soft x-ray energy range (1-20 keV) observed at ASDEX Upgrade are the superposition of bremsstrahlung and recombination continua with characteric line emission of typical intrinsic impurities like Si, Ar, Fe. The continuum spectrum has a characteristic exponential shape over the whole measurement range because additionally heated and dense ohmic plasmas are sufficiently thermalised in most cases.

The following information can be gained from the soft X-ray spectra without an absolute calibration: First of all, due to its high energy resolution SDD can be applied for the identification of intrinsic impurities having characteristic lines in the energy range of the diagnostic (Si through W). From the slope of the continuum spectra in a semi-logarithmic plot a fast guess of the central T_e can be gained [3]. By implementing an absolute calibration one obtains the possibility to measure the line brightnesses and hence, the concentrations of impurities using the impurity transport code STRAHL [4]. An analysis of a typical ASDEX Upgrade H mode discharge (#13595) showed concentrations of Fe and Ar of 370 ppm and 50 ppm, respectively. By fitting the strongest emission lines with a Gaussian function and subtracting them from the spectra one obtains the almost pure bremsstrahlung spectrum, because the contribution of recombination radiation is negligible under the usual discharge condition (no impurity accumulation). The effective ion charge Z_{eff} was determined by fitting the bremsstrahlung equation[3] $j(E) = 1.215 \cdot 10^{-36} n_e^2 \cdot \overline{g}_{ff} \cdot Z_{eff} \left(\sqrt{\frac{kT_e}{eV}}\right)^{-1} \cdot e^{-\frac{h\nu}{kT_e}}$ to the experimental spectra, where T_e and Z_{eff} are used as fit parameters. The line averaged electron density n_e is routinely measured by interferometry and normally used for the fit, because density profiles are mostly flat. The Maxwell averaged Gaunt factor $\overline{g}_{ff} = 1.5$ is known from literature. A simulation of incoming X-ray spectra at the SDD detector for a typical discharge was done, using the independently measured electron temperature and density profiles. A constant $Z_{eff} = 1.65$ was used for the reconstruction. As it shown in Fig.2 for these typical plasma temperatures and densities the line integrated emission registered by the detector is clearly dominated by the central plasma radiation, namely the plasma region within $\rho_{pol} = 0.35$. This means, that the PHA system is essentially a central plasma diagnostic. Comparison of independently measured $T_e(0)$ with T_e obtained from the fit to the bremsstrahlung shows, that the latter yields almost the real central temperature value (see Fig. 4a). For an improved H mode discharge # 14281 the line of sight integrated spectrum was reconstructed using the Zommerfeld Bremsstrahlung cross section and taking into account the electron temperature and density profiles under assumption of a fully thermalised plasma. The reconstructed spectrum shown in Fig. 3 together with the experimental one was obtained for the low field side $T_e(r)$, $n_e(r)$ and includes no effects of Shafranov shift and anisotropy. Even under these simple considerations the shape of the experimental spectrum is recon-

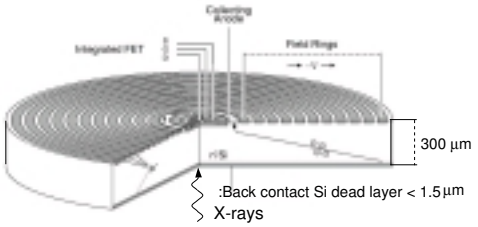

Figure 1. *Schematic view on cylindrical Silicon Drift Detector* [6].

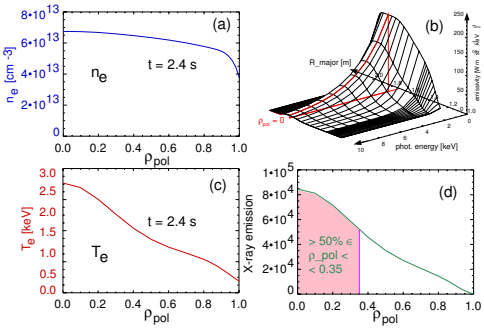

Figure 2. *Calculation of the bremsstrahlung in the energy range below 10 keV seen by the PHA diagnostic (b,d) from experimental $n_e(\rho_{pol})$ (a) and $T_e(\rho_{pol})$ (c) in discharge 13594 at t=2.4 s.*

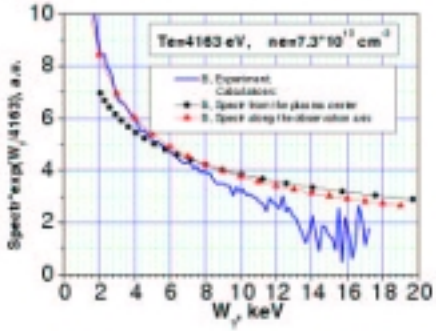

Figure 3. *Scaled experimental bremsstrahlung radiation in #14281 and its reconstruction either including the T_e and n_e (red dots) profiles or pure central radiation (black dots).*

structed for energies below 8 keV within the uncertainty of the measurements. The pure central plasma radiation, which is calculated with independently measured central temperatures, shows larger deviations from the experiment as compared to the LOS integrated spectrum.

In order to test the fit procedure for Z_{eff} a well diagnosed 1 MA H mode discharge of an established scenario was chosen, which is reproduced frequently to monitor long term changes of the plasma behavior and the machine conditioning. Z_{eff} was determined in three different time intervals: one with low n_e and low NBI heating power, and two with higher power at low and high electron densities. They correspond to three plateaus in T_e and almost constant plasma energy. Continuum emission from the plasma is recorded in the visible range as well. Z_{eff} from this line of sight averaged measurement (Fig. 4a bottom - red line) is used for a comparison with the results in SXR energy range, which are shown as blue bars in the lower part of Fig. 4a. The widths of the bars represent the time intervals for that the SXR spectra are accumulated. Inside the bars the electron temperatures from the fit are given (see also T_e plot). The temporal behavior as well as the absolute values of Z_{eff} from visible emission and from the SXR are in a good agreement.

In Fig. 4b the special feature of the PHA, namely its sensitivity to the central bremsstrahlung is presented for the discharge #13445. In this discharge peaked SXR emission profiles are observed by a one-dimensional unfolding [5] of the SXR brightness along approximately 30 chords. Fig. 4b shows the hollow SXR emission profile between 2.5 and 4 s, which then transiently goes through a normal emission profile and finally changes to a peaked one at approximately 4.5 s. Z_{eff} from the visible range radiation is relative insensitive to such changes in the emission profile shape. In contrast, the Z_{eff} from central SXRs follows roughly the central SXR emissivity. Additionally the data from the visible radiation show a good agreement with the variation of SXRs at the plasma edge. Beside of the normally measured SXR spectra, which lead to an exponential shape, spectra with high energetic tails were registered at ASDEX Upgrade (see Fig. 5). Most of non-plasma effects like pile-up, electronic noise as well as the line emission could be excluded from the consideration. Although the neutrons are able to cause a kind of contin-

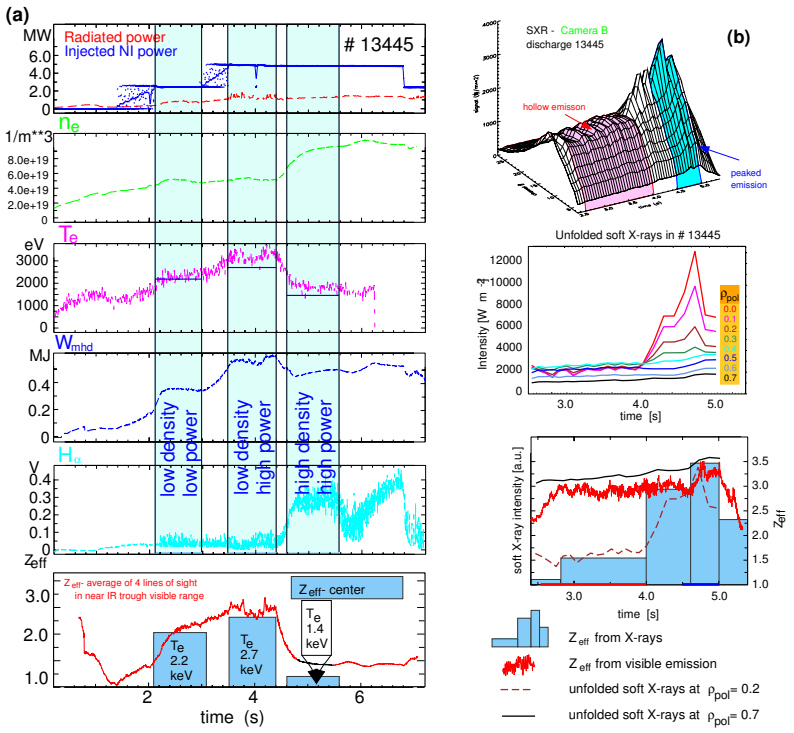

Figure 4. *(a) Comparison of the central (from X-ray, denoted with blue bars) and average (from visible emission, denoted with red line) Z_{eff} in the standard H mode discharge 13445. (b) In the H mode discharge 13920, where the emission profile changed from a hollow to a peaked one, Z_{eff} correlates with the central soft X-ray intensity.*

uum background signal, they, in certain cases are not able to explain the seen high energetic part of the spectra completely. These spectra can not be explained under the assumption of the pure Maxwell electron energy distribution function. So called slide away electrons are a possible explanation. These non thermalised electrons are proposed to be produced during the ECRH heated phases in low density plasmas. A distortion of the Maxwellian distribution by a longitudinal electric field was also considered [7]. Its magnitude was calculated with an electron kinetic equation with the linear Landau collisionality and non-relativistic bremsstrahlung cross-section. Indeed, these effects alone can not explain the observed high energy tails of the spectra. As it can be seen from Fig. 6 in the energy range of the SDD we are not able to measure deviations of spectra from the Maxwellian shape, if plasmas are observed along the chord crossing its center like it was actually done. Concerning the simulation data, just the line of sight observing the plasma far outside the center could allow to observe anisotropy effects due to $E_{||}$. This is indicated by the solid black line in Fig. 6, which shows the boundary kinetic energy for anisotropy effects. Roughly, the observation of deviations of spectra from Maxwellian shape are in principle possible, if spectra are measured in the energy range above the boundary energy (see Fig. 6). For this estimation typical measured longitudinal electric fields of approximately $0.02\frac{V}{m}$ at ASDEX Upgrade were taken into account. Experimental data show frequently high energetic tail during NBI with 100 kV beams. Horizontal Thomson scattering system sees simultaneously a sharp increase of parallel electron velocity in series of plasma discharges. This is probably just a few percent effect, because the measured bulk temperatures stay constant and are coincide with the standard T_e diagnostics. A production of high energy tails in the EEDF due to its interaction with high energy NBI were simulated with Fokker-Planck calculation and discussed in [8].

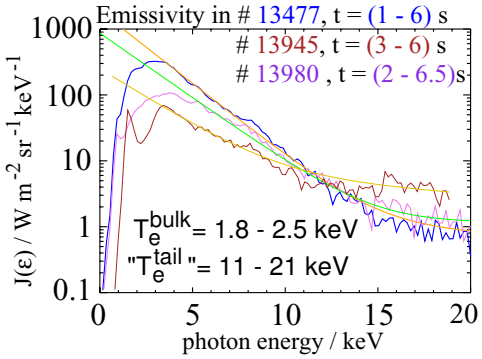

Figure 5. *Examples of high energy tails in the soft X-ray range.*

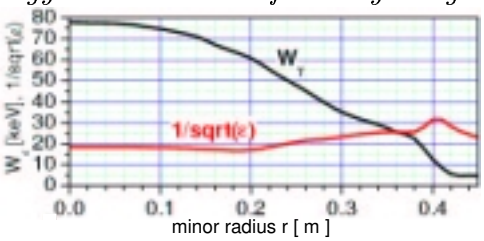

Figure 6. *The lower energy limit W_γ for anisotropy effects due to E-field in discharge #14281.*

Acknowledgment

The authors grateful to A. Kallenbach for supplying the empirical approximation for Z_{eff} in the visible range and J. Fink and M. Seth for technical assistance.

References

[1] L. Strüder et al., *Microsc. Microanal. 4, 622-631,* (2000).
[2] D. Bolshukhin et al., *submitted by Rev. Sci. Instr.* March 2001.
[3] I. Hutchinson, *"Principles of plasma diagnostics"*, Cambridge Univer. Press (1987).
[4] K. Behringer, *Internal JET Report, JET-R (87)08.*
[5] R. Dux, *private communications.*
[6] Ketek GmbH *http://www.ketek.net/Media/SDDdescription.pdf.*
[7] M. Kantor *Rev. Sci. Instr. 72, 1162-1165*, (2001).
[8] B. Kurzan et al., *this conf. P1.001*(2001).